Author for correspondence:

Bianca Maria Dinelli

e-mail: BM.Dinelli@isac.cnr.it

JUNO/JIRAM's view of Jupiter's H_3^+ emissions

B. M. Dinelli[1], A. Adriani[2], A. Mura[2], F. Altieri[2], A. Migliorini[2] and M.L. Moriconi[3]

[1]ISAC-CNR, Via Gobetti 101, Bologna - Italy
[2]IAPS-INAF, Via del Fosso di Cavaliere, Roma - Italy
[3]ISAC-CNR, Via Fosso di Cavaliere, Roma - Italy

The instrument JIRAM (Jovian Infrared Auroral Mapper), on board the NASA spacecraft Juno, is both an imager and a spectrometer. Two distinct detectors are used for imaging and spectroscopy. The imager acquires Jupiter images in two bands, one of which (L band, 3.3-3.6 μm) is devoted to monitor the H_3^+ emission. The spectrometer covers the spectral region from 2 to 5 μm (average spectral resolution 9 nm) with a 256 pixels slit, that can observe the same scene of the L band imager with some delay. JIRAM scientific goals are the exploration of the Jovian aurorae and the planet's atmospheric structure, dynamics and composition. Starting early July 2016 Juno is orbiting around Jupiter. Since then, JIRAM has provided an unprecedented amount of measurements, monitoring both Jupiter's atmosphere and aurorae. In particular the camera has monitored Jupiter's poles with unprecedented spatial resolution, providing new insights in both its aurorae and the polar dynamic. The main findings obtained by the L imager are detailed pictures of Jupiter's aurorae showing an extremely complex morphology of the H_3^+ distribution in the main oval and in the moon's footprints. The spectrometer has enabled to measure the distribution of both H_3^+ concentration and temperature. The analysis of the north auroral region limb observations shows that the peak density of H_3^+ is above 750 km and that often it is anticorrelated to the temperature, confirming the infrared cooling effect of H_3^+

1. Introduction

Since the discovery of its infrared spectrum by T.Oka in 1980 [1] and its identification in Jupiter's aurorae [2], H_3^+ has played an important role in the study of Jupiter's magnetosphere. Observations of the H_3^+ emission are now used to measure directly the auroral morphology of Jupiter and other giant planets, and also to investigate the magnetospheric conditions leading to the aurora formation. This observations are usually made in the near-infrared (3.4 μm) where a few emission lines of the H_3^+ ion are centred on a deep methane absorption band. In this spectral region the signal of Jupiter's ionosphere appear with extraordinary signal-to-noise ratio against a planet darkened by the absorption due to methane in its atmosphere [3]. Near Jupiter poles, the emissions of the main auroral oval are generated by the particle precipitation associated to the upward branch of the currents caused by the breakdown of the co-rotation of Jupiter and its plasma sheet, which is originated by the neutral gas emitted by Io's volcanos. Jupiter's aurorae also show H_3^+ emission features at the base of the magnetic field lines connecting the Galilean moons Io, Europa, and Ganymede to Jupiter surface. These emissions are known as the moons auroral footprints. H_3^+ emissions are thermally excited and are correlated to the precipitating particles energy deposition.

The importance of detailed observations of the H_3^+ emissions for the study of Jupiter aurorae has suggested the development of the Jupiter InfraRed Auroral Mapper (JIRAM) instrument [4], on board the NASA Juno satellite [5]. JIRAM is both an imager and a spectrometer and can acquire images in two spectral bands (one of which dedicated to H_3^+) and also measure spectra in the 2 to 5 μm region over a slit made of 250 pixels. The high resolution images of JIRAM in the 4.5 μm spectral band have enabled the identification of clusters of cyclones surrounding both Jupiter poles [6]. The images of the H_3^+ emissions have shown Jupiter's auroral regions with unprecedented details, observing North and South aurorae almost at the same time [7] and discovering that the Io footprint exhibits a spot structure and a split long tail [8]. JIRAM high resolution images of the H_3^+ emissions have also be compared to UltraViolet Spectrograph (UVS) observations of the North Aurora [9].

The spectrometer of JIRAM has enabled the mapping of the column density and temperature of H_3^+ for both north and south aurorae [10] [11] and the limb views of the H_3^+ spectrum in the mid-latitude and equatorial regions [12].

In this paper we will make a summary of the most important findings obtained by both the imager and the spectrometer of JIRAM obtained using H_3^+ emissions. The analysis of JIRAM data of the auroral region acquired during the first orbit around Jupiter will be discussed.

2. Instrument

JIRAM is both an imager and a spectrometer. It has been designed to study the aurorae of Jupiter, along with the atmospheric composition and dynamic. The imager focal plane is divided into two equal areas covered with two different filters: filter L, covering the 3.2 to 3.7 μm spectral region, and filter M, centered at 4.78 μm with a 480 nm bandwidth. The spectrometer's slit, made of 256 pixels, is located within the M filter field of view (FOV) and covers the 2–5 μm spectral interval in 336 spectral channels, all relative to the same instrumental view, with a spectral sampling of 8.9 nm. In the 3–4 μm spectral range each channel has a spectral resolution of about 12 nm. The instrument design allows imaging the auroral features both spatially and spectrally. As the spectrometer and the L band imager (designed to monitor the aurorae) are not colocated [13] the spectrometer measurements are planned to obtain an almost simultaneous observation of the same auroral region. On the rows of the bi-dimensional spectrometer sensor, the entrance slit (with a field of view of 3.5°) is covered by 256 pixels. The instantaneous field of view of each pixel is about 250×250 μrad. On the sensor column, the spectrum is sampled in 336 spectral channels with integration time of 30 s.

Due to the distance of the Juno spacecraft from Jupiter, JIRAM FOV does not allow to cover the entire polar region in a single image during the polar overpasses. However, JIRAM's scanning mirror can be used to cover most of the auroral features. About 25 images are merged into a mosaic to give a comprehensive image of the aurora and satellite footprints. The mosaics are assembled processing the data to remove the contamination due to strong signals present in the companion M band detector [7] and averaging the best available data where the single images overlap.

The spectrometer usually observes Jupiter in nadir geometry; limb observations are acquired whenever the spectrometer slit samples the region right above Jupiter's limb, above the 1 bar level surface. Unfortunately their location cannot be planned in advance, due to the constraint posed by the spacecraft orientation and of the JIRAM location within the spacecraft. Each JIRAM pixel is geo-referenced in System III planetocentric geographical coordinates, using the NAIF-SPICE tool [14]. For the limb views, the corresponding pixels are geo-referenced using the tangent point, that is the location where the instrument line of sight (LOS) reaches the minimum distance with the 1-bar surface of Jupiter. Each tangent point is characterised by the tangent altitude, that is the value of the minimum distance to the 1 bar level surface and by the latitude and longitude of the point where the normal to the LOS at the tangent point crosses the same surface. We refer to each set of limb observations belonging to the same slit acquisition, as a 'limb sequence' or 'limb scan'. The uncertainty in the spacecraft pointing reconstruction (of the order of 0.01 s) and of the scanning mirror motion translates in the precision of the geometric information, which is correct within 1 pixel, and the spatial resolution of 1 pixel depends on the distance between the aircraft and the 1 bar Jupiter surface.

3. Observations

JIRAM has observed Jupiter in many orbits, here we report and discuss the observations made during the first Juno orbit, when JIRAM observations thoroughly covered both the northern and southern auroral regions. The observations were acquired on 27 August 2016. The aurora was observed by both the imager and the spectrometer; the north aurora from 08:24 to 11:51 UTC and the south aurora from 15:00 to 19:45 UTC. The spatial resolution of the spectrometer at the 1 bar level ranged between 45 and 135 km, while the resolution of the imager ranged from 90 to 20 km/pixel for the north aurora and 50 to 130 km/pixel for the south aurora.

If figures 1 and 2, in the left panel, we report a superimposition of the images acquired with the L band imager of the north and south polar regions respectively. The figures show the complexity of Jupiter's aurorae. In the same figures, in the right panels, the coverage of the slit of the spectrometer is shown. The colours of the pixels represents the integrated intensity of the spectral region from xx to yy microns.

The coverage of the spectrometer has been quite extensive in the auroral region from latitudes around 60 poleward. From the figures we see that the spectrometer integrated intensity reflects what the imager has observed. However the details of the auroral morphology are better resolved with the images, due to the higher spatial sampling obtained by the 2-D detector of the imager. However despite the coarser sampling of the spectrometer, the possibility to resolve spectrally the auroral signal enables to measure both the H_3^++ density and its temperature. If the spectrometer slit has the right orientation, we can also observe the auroral region in limb geometry. In the first Juno orbit we have been lucky enough to have few spectra measuring the north auroral region in limb geometry. This will enable to evaluate the vertical distribution of the H_3^++, with important links to the extent of the penetration of the particles that generates the H_3^++ formation. No limb observations are available for the south aurora.

The north aurora has a sharp appearance in the longitude region from 150 to 240 longitude, while we see a broad region of enhanced emission in the remaining part of the oval. The integrated intensity over the H_3^+ spectral region observed by the spectrometer confirms this behaviour. The diffuse central bright area coincide (?) with the methane emission identified by Moriconi et al. [15] while the two bright spots do not have any correlation with methane.

The south aurora appears significantly brighter at the time of our observations. We see diffuse emission spots, possibly signatures of the plasma injection [16], outside the main oval that may be linked to similar features in the north aurora; [Mauk et al., 2002; Dumont et al., 2014].

The main ovals (both south and north) are made of a narrow single arc for half of it and multiple arcs plus broad diffuse emissions in the other half. The diffuse region shows multiple structures of coherent pattern that may map the closed field line region of Jupiter's magnetosphere. However similar features are not present in the south, observed however about 10 h later. The unprecedented spatial resolution of JIRAM shows that the thickness of the single arc region is 500 km in the south and 700 km in the north.

4. Analysis and results

The analysis of the acquired spectra in nadir geometry has been reported by Dinelli et al [10] for the north aurora and by Adriani et al [11] for the south aurora. The observations in limb geometry have been analysed using the same code described in Migliorini et al. [12] Here we briefly recall both the analysis methods. The retrievals have been performed using a Bayesan approach. In the case of Nadir observations we have analysed each spectrum singularly simulating both H_3^+ and CH_4 emissions with the espression reported in [10]. In the case of limb observations we have analysed all the spectra of a limb sequence simultaneously, using the global fit technique [17]. The spectra have been simulated using a line by line full physics radiative transfer code that takes into account all the absorption and emission processes along the line of sight of the instrument. No scattering was included. The free parameters of the retrievals were the H_3^+ column density (CD) and temperature in the case of nadir observations and the vertical distribution of the H_3^+ Volume Mixing Ratio (VMR) and temperature in the case of limb observations. Since the H_3^+ signal in the auroral region can be observed in the spectra with tangent altitudes up to 1100 km, the retrieval of both T and H_3^+ VMR have been performed from 450 to 1050 km at 100 km step. We have discarded the spectra at lower altitudes because of contamination of the spectra by methane emission and scattering effect.

Figure 3 shows the results obtained for the north auroral region and figure 4 the results for the south auroral region using the nadir observations only. A thorough discussion of these results can be found in [10] and [11]. Comparing the maps we see that while the H_3^+ CD has peak values along the predicted auroral path in both north and south aurorae, the peak temperature shows different behaviour in the two poles. While in the north the temperature peak has an oval pattern similar but not supeimposed to the CD oval, in the south the temperature peak is more widely distributed; however the distribution of high temperature never coincide with the peak CD. This suggests that probably the high CD oval is produced by high-energy electrons that penetrate deep in the atmosphere, where the temperature is lower, while less energetic electrons will stop at higher altitudes, and generate H_3^+ in the upper layers of the atmosphere, where the temperature is larger [18]. Another explanation could be that large H_3^+ CDs lead to a large infrared cooling of the surrounding atmosphere as suggested by Miller et al. [21]. However there is not a clear anticorrelation between temperature and CD, suggesting that only the thermostat mechanism cannot explain the observed behaviour. Both emissions and temperatures retrieved from the southern aurora are significantly higher than the ones observed in the north. This could be linked to the combination of the asymmetry in the location of the magnetic poles with respect to the planet rotation axis and the circulation of hydrogen in the upper atmosphere. The observed north-south temperature difference agree with model predictions.

Figure 5 shows the CD map of the North auroral region with superimposed stars that show the averaged location of the limb scans found in two spectrometer images sampling the auroral regions. We will refer to the topmost series as image 1 and to the other series as image 2. Unfortunately the two images sample regions of the north aurora that have not been thoroughly sampled by the nadir observations. Figure 6 and 7 report the results of the analysis of the limb observations for image 1 and 2 respectively. All the maps report the quantities as a function of altitude (y axis) and of the averaged latitude of the limb sequences (x axis). In each figure the

top left panel shows the integrated intensity of the analysed spectra, the top right panel the retrieved VMR, the bottom left panel the retrieved temperature and the right bottom panel the concentration of H_3^+ obtained combining the retrieved temperatures and VMR using the pressure profile assumed in the retrievals.

The top left panel of Figure 6 shows that the integrated emissions of H_3^+ varies dramatically from regions outside to region above the auroral main oval. In particular we see a peak of the intensity in the spectra with tangent altitudes from 650 to 950 km above the 1 bar surface of Jupiter. The same panel of figure 7 shows a similar increase but homogeneously distributed over the whole vertical range of the observations. This difference is not reflected in the top right panels of the two figures, that show the maximum of the H_3^+ retrieved VMR from the observed spectra with approximately the same vertical distribution (maximum above 700 km). The behaviour of the integrated emission reported in figure 7 can be explained by the fact that in limb geometry the signal reaching the instrument is due to the signal originated by all the atmospheric layers encountered by the instrument LOS. In case the atmosphere is optically thin, we attribute to the tangent altitude of the observations the signal that can be originated by layers well above the tangent altitude layer. The retrieval code however, representing correctly the physical processes occurring along the LOS, enables to retrieve the correct distribution of the H_3^+ density.

The lower left panels of figure 6 showing the retrievd temperatures, and the lower right panels of the same figure, showing the H_3^+ concentration (mol/cm^3), show that there is an anticorrelation between the peak density of H3+ and the higher temperature region. This is confirmed by the same panels of figure 7. In this last figure we also see that the high H_3^+ density at the rim of the auroral oval tends to extend to lower altitudes producing a sort of 'wall' that separates the polar regions from the mid-latitude regions. The comparison between H3+ density distribution and temperature distribution suggests that in the examined region the mismatch between the temperature oval and the density oval are due to the infrared cooling effect of H_3^+, more than in the altitude location of the H_3^+ peak density.

The peak density of H3+ in the auroral oval is always above 750 km, but not negligible values can be found also at lower altitudes, often at the borders of the auroral arcs.
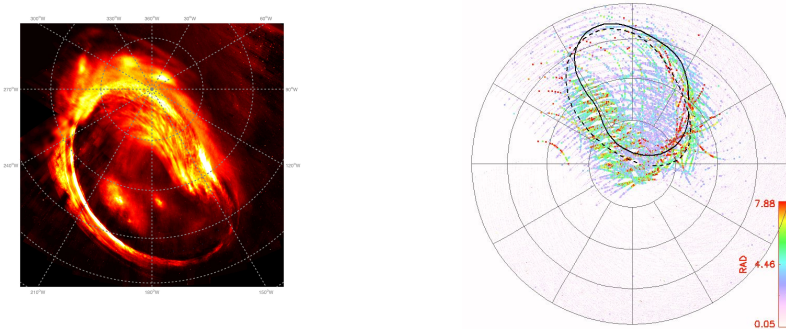
5. Figures & Tables

Figure 1. Jupiter north aurora as observed by the imager (left panel), and the spectrometer (right panel)
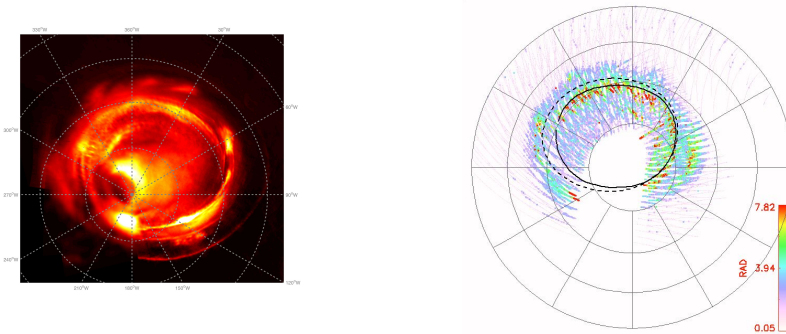

Figure 2. Jupiter south aurora as observed by the imager (left panel), and the spectrometer (right panel)
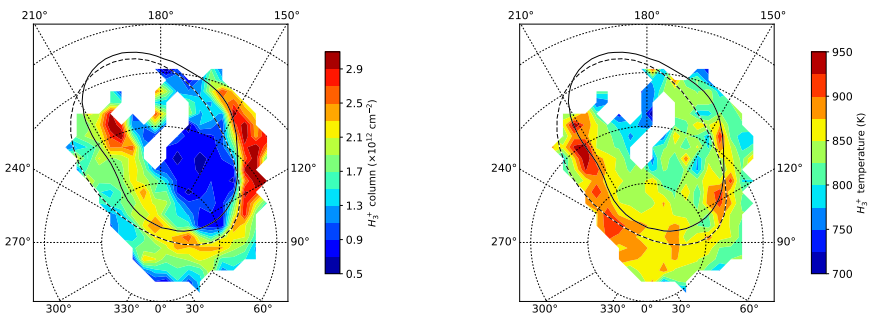

Figure 3. Jupiter north aurora H_3^+ column densities (right panel) and temperature distribution (left panel)

6. Conclusion

During the firts orbit of Juno around Jupiter, JIRAM observed both the north and south auroral regions with a short time delay. The north and south aurorae have been mapped by both the
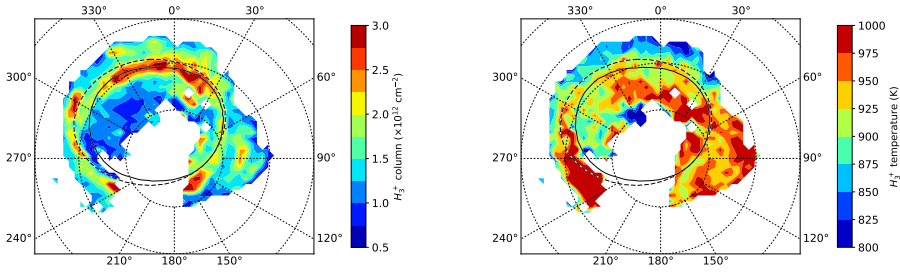
Figure 4. Jupiter south aurora H$_3^+$ column densities (right panel) and temperature distribution (left panel)
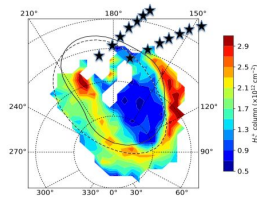

Figure 5. Jupiter north aurora CD map with superimposed the location of the analysed limb scans (black stars)

spectrometer and the L band imager with umprecedented spatial resolution. High-resolution images of both poles show very thin structures (few hundreds of kilometers) and diffuse structures. The intensity of the north aurora H3+ emission is lower than the south aurora one. The thickness of the single auroral arc is about 500 km in the north and 700 km in the south. The analysis of the spectrometer data acquired in nadir geometry has enable to obtain both CD and temperature of H$_3^+$. We have seen that at both poles the peak H$_3^+$ CD oval does not superimpose to the peak temperature one. The analysis of the few limb observations of the north auroral region show that the peak density of H$_3^+$ is always higher than 750 km above the 1 bar surface of Jupiter. We have also seen that the high H$_3^+$ density at the rim of the auroral oval tends to extend to lower altitudes producing a sort of 'wall' that separates the polar regions from the mid-latitude regions. Temperature and density are often anticorrelated, confirming the infrared cooling effect of H$_3^+$.

Ethics.

Data Accessibility. Insert details of how to access any supporting data here.

Authors' Contributions. AA is JIRAM PI and together with AM is responsible for the imager and spectrometer data. FA, AM, and MLM performed the data selection. BMD performed the data analysis, and drafted the manuscripti. All auhtors read and approved the manuscript.

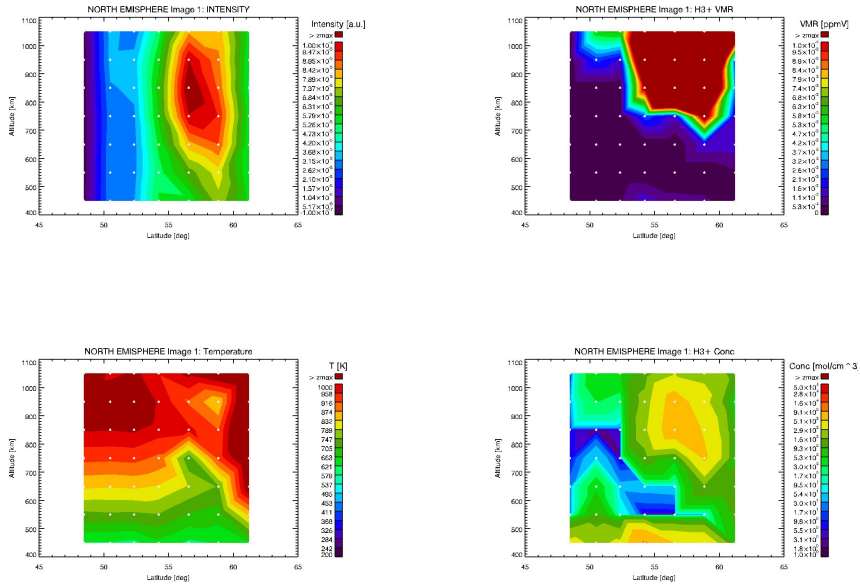Competing Interests. The author(s) declare that they have no competing interests.

Figure 6. top left panel: integrated intensity of the image 1 spectra, top right panel: retrieved VMR, bottom left panel: retrieved temperature and right bottom panel: concentration of H_3^+ (mol/cm^3) for image 1. All the maps report the quantities as a function of altitude (y axis) and of the averaged latitude of the limb sequences (x axis).
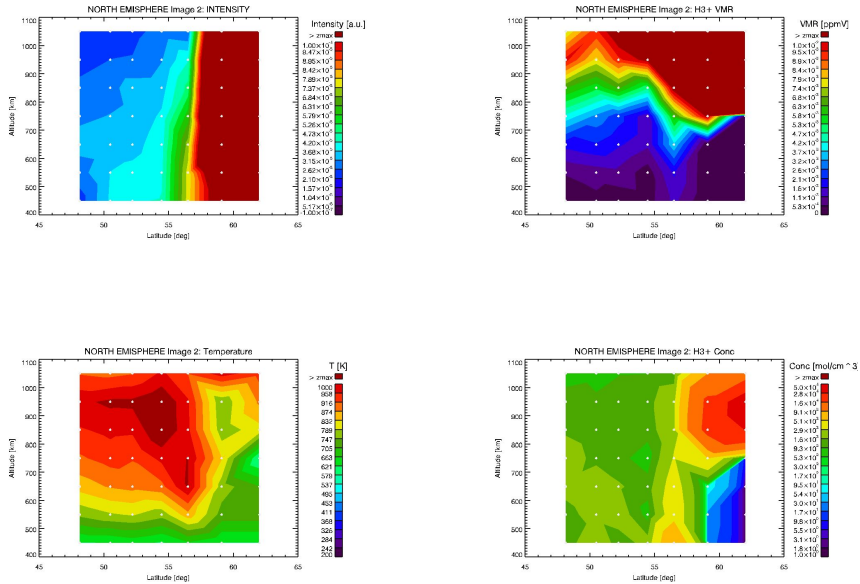

Figure 7. Same as figure 6 but for image 2

References

1. Oka T. 1980. Observation of the Infrared Spectrum of H+3 *Physical Review Letters* **45** 531–534
2. Drossart, P. et al. 1989. Detection of H+3 on Jupiter *Nature* **340** 539–541, doi:10.1038/340539a0
3. Connerney J.E.P. and Satoh (2000) The H_3^+ ion: a remote diagnostic of the jovian magnetosphere *Phil. Trans. R. Soc. Lond. A* **358** , 2471-2483, doi:10.1098/rsta.2000.0661
4. Adriani A., et al. 2017. JIRAM, the Jovian Infrared Auroral Mapper *Space Sci. Rev.* **213** 393-446, doi:10.1007/s11214-014-0094-y.
5. Bolton S. J., et al. 2017. The Juno MIssion *Space Sci. Rev.* **213** 1–3, doi:10.1007/s11214-017-0430-6.
6. Adriani A., et al. Clusters of cyclones encircling Jupiter's poles *Nature* **555** 216-219, doi:10.1038/nature25491.
7. Mura A. et al. 2017. Infrared observations of Jovian aurora from Juno's first orbits: Main oval and satellite footprints *Geophys. Res. Lett.* **44** 5308–5316, doi:10.1002/2017GL072954
8. Mura A. et al. 2018. Juno observations of spot structures and a split tail in Io-induced aurorae on Jupiter *Science*, doi:10.1126/science.aat1450
9. Gérard J.-C. et al. 2018. Concurrent ultraviolet and infrared observations of the north Jovian aurora during Juno's first perijove, *Icarus* **312** 145-156, doi:10.1016/j.icarus.2018.04.020
10. Dinelli B.M. et al. 2017 Preliminary JIRAM results from Juno polar observations: 1. Methodology and analysis applied to the Jovian northern polar region *Geophys. Res. Lett.* **44** 4625-4632, doi:10.1002/2017GL072929.
11. Adriani A. et al. 2017 Preliminary JIRAM results from Juno polar observations: 2. Analysis of the Jupiter southern H_3^+ emissions and comparison with the north aurora *Geophys. Res. Lett.* **44** 4633-4640, doi:10.1002/2017GL072905.
12. Migliorini a. et al. 2019.
13. A. Adriani et al. (2014) JIRAM, the Jovian Infrared Auroral Mapper. *Space Sci. Rev.* doi:10.1007/s11214-014-0094-y
14. Acton C.H. 1996 Ancillary data services of NASA's navigation and ancillary information facility *Planet. Space Sci.* **44** 65-70, doi: 10.1016/0032-0633(95)00107-7.
15. Moriconi M.L. et al. 2017
16. Dumont et al., 2014 Jupiter's equatorward auroral features: Possible signatures of magnetospheric injections, *J. Geophys. Res. Space Physics* **119**, 10,068–10,077, doi:10.1002/2014JA020527.
17. Carlotti M.L. et al. 1990
18. O'Donoghue, J., et al. (2014), Conjugate observations of Saturn's northern and southern aurorae, *Icarus*, **229**, 214–220, doi:10.1016/j.icarus.2013.11.009.
19. Grodent, D., J. H. Waite Jr., and J.-C. Gèrard (2001), A self-consistent model of the Jovian auroral thermal structure,*J. Geophys. Res.* **106**, 12,933–12,952, doi:10.1029/2000JA900129.
20. Hiraki, Y., and C. Tao (2008), Parameterization of ionization rate by auroral electron precipitation in Jupiter, *Ann. Geophys.*, **26**, 77–86, doi:10.5194/angeo-26-77-2008.
21. Miller, S., et al. (2013), Cooling by emission, *J. Phys. Chem. A*, **117**, 9770–9777, doi:10.1021/jp312468b.